Journal of Chromatography, 218 (1981) 123–135
Elsevier Scientific Publishing Company, Amsterdam — Printed in The Netherlands

CHROM. 14,230

EFFECT OF RADIAL THERMAL GRADIENTS IN ELEVATED TEMPERATURE HIGH-PERFORMANCE LIQUID CHROMATOGRAPHY

S. ABBOTT*, P. ACHENER, R. SIMPSON and F. KLINK

Varian Associates Instrument Group, Walnut Creek Division, 2700 Mitchell Drive, P.O. Box 9016, Walnut Creek, CA 94598 (U.S.A.)

SUMMARY

The advent of highly efficient columns in high-performance liquid chromatography (HPLC) requires careful design of extra-column components such as injectors, coupling tubing and detectors in order to minimize peak dispersion. A dispersion effect which has not been treated in detail in the chromatographic literature is that of a radial thermal gradient at the column inlet generated by an imbalance between the inlet fluid and column temperature. The significance of this effect and a means to reduce it in elevated temperature HPLC is demonstrated in this report.

INTRODUCTION

A potential limit to achieving the separation efficiency inherent to an high-performance liquid chromatographic (HPLC) column is the variance due to a mismatch of the temperature of the mobile phase entering the column and the column temperature. Typical HPLC solvents and packings such as silica and polystyrene are poor thermal conductors relative to stainless steel. Thus, the fluid segment entering the wall region of the column will come to the column set temperature before the fluid segment entering the center of the column. The resultant radial thermal gradient translates into a radial retention gradient and hence into solute band broadening.

THEORETICAL

A detailed theoretical treatment of a radial thermal gradient in a column, generated by a mismatch of inlet fluid and column temperatures is given in Appendix I. The radial thermal gradient, $T_{center} - T_{wall}$, should be dependent on the difference between the inlet fluid and column temperature, the flow-rate and column bore and should be essentially independent of the mobile phase, the particle size of the packing and the solute.

The theoretical treatment of Appendix I predicts that radial thermal gradients can be minimized by reducing the column bore (decreases with the second power of the column bore) and by heating the mobile phase to the column temperature prior to the column inlet. The success of the latter procedure is demonstrated later in this report.

0021-9673/81/0000–0000/$02.50

The variance due to the presence of a radial thermal gradient in an HPLC column is a complex function of several factors. Since the temperature at the column center will be lower than that at the walls, the center fluid will have a higher viscosity, η, and thus center molecules will not only experience a higher capacity factor, k', but a lower flow velocity, u, and different eddy diffusion and mass transfer plate heights than do wall molecules. These radial effects should lead to increased peak dispersion.

The degree to which a centrally injected solute band diffuses out towards the column walls during its migration through the column will determine the degree to which it "sees" the radial thermal gradient. A centrally injected sample slug and a smaller particle size[1] packing should decrease outward diffusion of the solute band and thus reduce the the variance observed for a given radial thermal gradient.

One should also note that frictional heating of the mobile phase produces a radial thermal gradient opposite in direction to that of the inlet fluid/column temperature mismatch. The magnitude of this effect has been shown by Halasz *et al.*[2] to increase linearly with operating pressure.

Factors which determine the degree to which a radial thermal variance affects chromatographic performance are the column plate height and column length. Since radial thermal gradient and column plate heights are additive, the effect of a given radial thermal gradient variance on chromatographic performance will increase as column plate height is reduced. The fraction of the column in which the radial thermal gradient is significant increases as column length decreases. The theoretical treatment of Appendix I predicts that the radial thermal gradient is significant over the initial 1.5–2.5 cm of a typical column. Thus, use of shorter columns such as 5–10 cm should increase the effects of radial thermal variances over those seen with 15–30 cm columns.

EXPERIMENTAL

Chromatography was performed using a Varian Model 5060 liquid chromatograph and a Varian UV-50 variable-wavelength detector having an 8-μl flow cell and selectable time constants of 2, 1, 0.5 sec. Injections (2 μl) were made using a six-port Valco sample injection valve with a 10-μl loop. The 13% C moderate loading C_{18} reversed-phase columns used were Varian MicroPak MCH-10 (4 × 300 mm) and MicroPak MCH-5 (4 × 150 mm). The inlet mobile phase was pre-heated between the injector and column, using an aluminum bar in which two slots were milled, to hold a 10-cm loop of 0.23 mm I.D., 316 stainless-steel tubing. The bar was placed in the A side of the Model 5060 column heater, and connected via a 5 cm × 0.23 mm I.D. tube to the analytical column in the B side of the heater. The 5-cm connector was insulated with a short piece of refrigeration tubing.

RESULTS AND DISCUSSION

Radial thermal gradients in reversed-phase chromatography (RPC) of non-polar solutes

The chromatographic consequences of a radial thermal gradient are shown in the experimental plate height–temperature data of Fig. 1, obtained on 4 × 300 mm MCH-10 (10-μm C_{18}) and 4 × 150 mm MCH-5 (5-μm C_{18}) columns. Data was taken

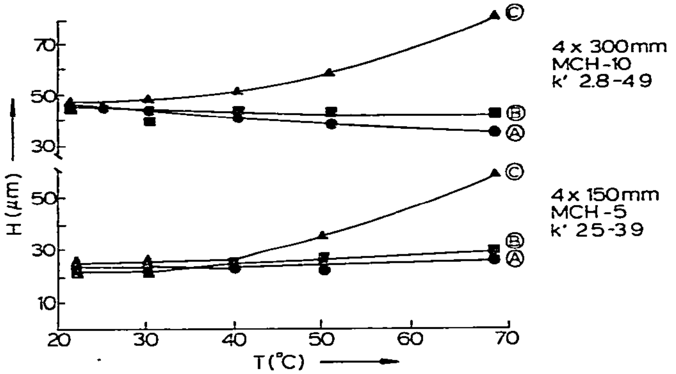

Fig. 1. RPC of anthracene. Temperature dependence of plate height: A, theoretical prediction (see Appendix III). B, experimental data, with inlet mobile phase heated to column T with preheater loop; C, experimental data, without pre-heating of inlet mobile phase. Lower section is data for 4 × 150 mm MicroPak MCH-5. Upper section is data for 4 × 300 mm MicroPak MCH-10. Mobile phase: 70% acetonitrile in water; flow-rate 1 ml/min.

with and without heating of the mobile phase to the column temperature prior to the column inlet. The "pre-heating" was achieved simply by fixing a 10-cm loop of 0.23 mm I.D. tubing in an aluminum bar which was placed in one compartment of the Model 5060 dual column heater. Calculation of the tubing length necessary to pre-heat the mobile phase to a given temperature at a given flow-rate, is described in Appendix II. The heated loop was connected to the column, located in the second compartment of the column heater, via a 5 × 0.23 cm tubing length which was insulated with a short piece of refrigeration tubing.

The 10-μm C_{18} traces of Fig. 1 represent a theoretical prediction of $H(T)$, as described in Appendix III (Trace A); experimental $H(T)$ data, using pre-heated mobile phase (Trace B); and experimental $H(T)$ data, without pre-heating of the mobile phase (Trace C).

The experimental data demonstrate the efficacy of the pre-heater loop in that its experimental $H(T)$ curve matches the theoretical $H(T)$ curve up to 50°C, the

TABLE I

RADIAL THERMAL GRADIENT PLATE HEIGHT CONTRIBUTIONS

Non-polar solute: anthracene. Mobile phase: 70% acetonitrile in water; flow-rate 1 ml/min. Column: MicroPak MCH-10 (10-μm C_{18}), 4 × 300 mm.

Plate height term	*Contribution (μm)*	
	30°C (k' 4.9)	*50°C (k' 3.7)*
Column	47	42
H_T, radial thermal gradient (uncorrected)	4.8	14.9
Pre-heater loop for elimination of H_T*	0.41	0.46

* Theoretical estimate based on treatment of ref. 3.

normal operating range of silica-based HPLC columns. The deviation between curves B and C at $T > 50°C$ may indicate increased radial diffusion of the solute band rather than a radial thermal gradient effect. The reduction in plate height with temperature is due to dominance of the eddy diffusion and mobile phase diffusion terms which are proportional to $D_m^{-0.33}$ and $D_m^{-1.0}$ respectively, where the mobile phase diffusion coefficient, D_m, is proportional to T/η (η = viscosity).

Curve C, representing $H(T)$ without the pre-heater loop demonstrates the consequences of a radial thermal gradient. The plate height increase is significant above $\approx 25°C$. The difference between the B and C curves can be taken to be the radial thermal gradient plate height, H_T. The data of Table I shows that at 30°C and 50°C, the thermal term H_T is highly significant. These experimental values are compared to theoretical estimates of variance due to laminar flow through the pre-heater loop (based on treatment of ref. 3).

The data of Fig. 1 suggests that optimum operation of the 10-μm column for RPC of non-polar compounds would be at a temperature $\approx 10°C$ above ambient in order to control column T and thus optimize retention reproducibility, and obtain $\approx 10\%$ lower plate height. Higher temperature does not significantly reduce the plate height. Thus, 30–40°C operation with a pre-heated mobile phase is recommended for 10-μm RPC of non-polar compounds.

The 5-μm C_{18} traces of Fig. 1 again demonstrate the efficacy of the pre-heater loop in that its experimental curve matches the theoretical prediction of $H(T)$. The relatively flat H *versus* T curve was predicted due to the fact that in reducing particle size to 5 μm, the mobile phase diffusion term loses relative significance and the eddy diffusion and longitudinal terms, which are proportional to $D_m^{-0.33}$ and $D_m^{+1.0}$ gain significance.

The C curve of the 5-μm data indicates that up to 40°C, the thermal plate height H_T is relatively small (≈ 1.5 μm). This may be due to increased frictional heating of the mobile phase, which could balance the inlet fluid/column temperature thermal gradient and to the reduced degree of solute diffusion to the walls with the 5-μm particle bed. The 5 μm, 15 cm column operated at $\approx 2.6\times$ the pressure of the 10 μm, 30 cm column and thus should have a 2.6 fold greater degree of frictional heating.

The H_T term (B minus C curves) becomes significant above 40°C, presumably due to the simultaneous decrease in frictional heating due to reduced operating pres-

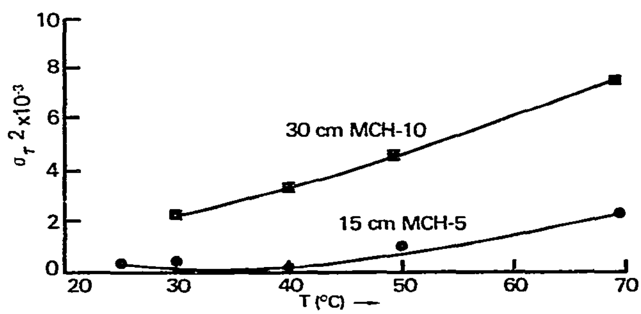

Fig. 2. Variance due to radial thermal gradient, σ_T^2, as function of temperature for 4 × 150 mm MicroPak MCH-5 and 4 × 300 mm MicroPak MCH-10 columns. Details as in Fig. 1. Note: in absence of secondary effects, σ_T^2 would be equivalent for the columns.

TABLE II

RADIAL THERMAL GRADIENT PLATE HEIGHT CONTRIBUTIONS

Conditions as in Table I, except for MicroPak MCH-5 (5-μm C_{18}), 4 × 150 mm.

Plate height term	*Contribution (μm)*	
	30°C (k' 3.7)	*50°C (k' 2.9)*
Column	20	20
H_T, radial thermal gradient (uncorrected)	1.5	11.5
Pre-heater loop for elimination of H_T*	1.3	1.3

* Theoretical estimate based on treatment of ref. 3.

sure, the increase in solute band diffusion to the walls due to increased D_m and the increasing radial thermal gradient. However, the 5-μm H_T values are still significantly less than one would predict in the absence of the secondary effects of frictional heating and reduced radial diffusion. This fact is shown clearly in Fig. 2, a plot of radial thermal gradient variance, σ^2_T, *versus* temperature for the 10-μm and 5-μm RPC columns. The σ^2_T values for the 5-μm column are 5–10 fold lower than those of the 10-μm column in the 25–50°C operating range.

The data of Table II indicates that heating of the 5-μm column will not significantly reduce plate height, and that operation slightly above ambient (25–30°C) with a pre-heated mobile phase, in order to optimize retention reproducibility (due to column *T control*) is optimum. The pre-heater loop can be reduced to less than 5 cm for this low *T* operation.

Radial thermal gradients in reversed-phase chromatography of ionic compounds

Reversed-phase plate heights of ionic solutes are significantly larger than those observed for non-polar solutes. The increased plate height of an ionic compound is

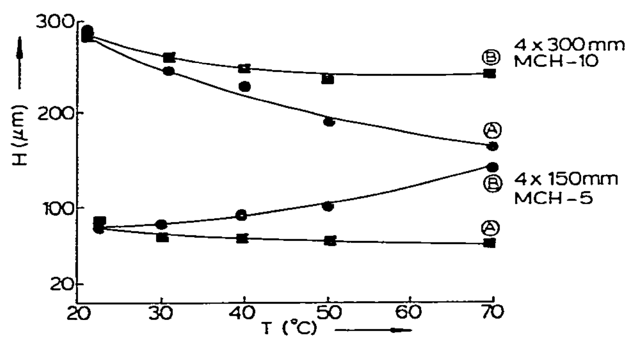

Fig. 3. RPC of quinidine. Temperature dependence of plate height: A, experimental data, with inlet mobile phase heated to column *T* with pre-heater loop. B, experimental data, without pre-heating of inlet mobile phase. Mobile phase: 90% aqueous KH_2PO_4 buffer (0.02 *M*, pH 2), 10% acetonitrile, 0.02 *M* in tetramethylammonium chloride (competing base); flow-rate 1 ml/min.

presumably due to slower mass transfer in the stationary and/or mobile phase. These processes are dependent on the first power of the diffusion coefficient. Thus, the plate height of an ionic solute such as the base quinidine should decrease more rapidly with an increase in column temperature than does that of a non-polar solute such as anthracene. This effect is shown in the experimental data of Fig. 3. Again, one notes that the use of a pre-heated mobile phase provides a significant reduction in observed plate height.

The data of Fig. 3 suggests that optimum ionic RPC operation should be at ≈35–50°C to reduce plate height by 20–40% for 10-μm and 10–20% for 5-μm columns. Higher temperatures can result in a significant reduction in column life due to increased rate of silica dissolution by aqueous RPC buffers. As is the case for non-polar solutes, mobile phase pre-heating is recommended for elevated temperature RPC of ionic solutes.

CONCLUSIONS

An imbalance between the inlet fluid temperature and the column temperature should generate a radial thermal gradient in the initial 1.5–2.5 cm of a 4 mm I.D. reversed-phase column. Peak dispersion in RPC due to a radial thermal gradient has been shown to be significant for 4 mm × 15–30 cm columns and has been shown to be greater for the case of 10-μm particles than for 5-μm particles. The latter observation may be due to the action of secondary effects such as frictional heating, which creates a radial thermal gradient opposite in direction to that generated by an inlet fluid/column temperature imbalance; and reduced radial diffusion of a centrally injected slug outwards to the walls with the smaller particles.

The use of a short "pre-heater" loop of 0.23 mm I.D. tubing in the column thermal block has been demonstrated to be effective in reducing the radial thermal gradient effect. A theoretical treatment of temperature gradients in packed columns (Appendix I) indicates an exponential decrease in the radial thermal gradient as column bore decreases, predicting that this dispersion effect should be significantly reduced with future microbore (*e.g.*, 1 mm I.D.) packed columns.

APPENDIX I

Theoretical treatment of temperature gradients in packed columns

The mechanism of heat transfer in packed cylinders has been studied, both experimentally and theoretically, by a number of investigators. One of the most successful analyses was developed by Singer and Wilhelm[4] who obtained an analytical solution and applied it to the data of Leva[5], Leva and Grummer[6] and others. The result of these authors for the temperature distribution in a cylindrical geometry is

$$\frac{\theta_f}{\theta_o} = \sum_{1}^{\infty} \frac{2}{\beta_n J_1(\beta_n)} \cdot J_o \cdot \left(\beta_n \frac{r}{R}\right) \cdot \exp\left(-4\beta_n^2 E_n \chi / D\right) \tag{A1}$$

where

$\theta_f = t_w - t_f =$ (wall temperature) $-$ (fluid temperature along the column), °C
$\theta_o = t_w - t_o =$ (wall temperature) $-$ (entrance temperature of fluid), °C
J_o and J_1 = Bessel functions of zero and first order respectively
β_n = nth root of $J_o(\beta)$
$R = D/2$ = inner radius of tube, cm
r = radius in the cylindrical coordinate system, cm
χ = axial coordinate

$$E_n = \left[\frac{1}{(\text{Pe})_o \dfrac{K_f}{K_{e,s}} + S_n} + \frac{\sigma}{(\text{Pe})_o} + \frac{1}{(\text{Pe})_{\varepsilon,0}}\right]\frac{D_p}{D} \qquad \text{(A2)}$$

where

$(\text{Pe})_o$ = a reduced Pe'clet number = $U_o D_p/\alpha_f$
$(\text{Pe})_{\varepsilon,0}$ = a reduced and modified Pe'clet number = $U_o D_p/E$
U_0 = superficial velocity that would exist if the tube were empty, cm/sec
D_p = particle diameter, cm
α_f = thermal diffusivity of the fluid, cm^2/sec
ε = eddy diffusivity, cm^2/sec
σ = void fraction between particles
S_n = a dimensionless quantity which can be shown to be negligible in the cases of interest in the present study
$K_{e,s}$ = an equivalent thermal conductivity for the combined fluid and the solid particles, cal/cm · sec · °C
K_f = (true) thermal conductivity of the fluid, cal/cm · sec · °C

then E_n reduces to:

$$E = \left[\frac{K_{e,s}}{(\text{Pe})_o K_f} + \frac{\sigma}{(\text{Pe})_o} + \frac{1}{(\text{Pe})_{\varepsilon,0}}\right]\frac{D_p}{D} \qquad \text{(A3)}$$

Inserting numerical values for β_n and J_1 in eqn. A1 gives the following equation for the temperature distribution:

$$\frac{\theta_f}{\theta_o} = 1.602\, J_o\left(2.405\,\frac{r}{R}\right) e^{-23.13 E_\chi/D} - 1.065\, J_o\left(5.52\,\frac{r}{R}\right) e^{-121.9 E_\chi/D} +$$

$$+ 0.851\, J_o\left(8.65\,\frac{r}{R}\right) e^{-299.5 E_\chi/D} - 0.730\, J_o\left(11.79\,\frac{r}{R}\right) e^{-566 E_\chi/D} + \cdots \qquad \text{(A4)}$$

To apply this equation, the dimensionless parameter E must be first evaluated and this requires that $K_{e,s}$, the equivalent thermal conductivity of the combined liquid and solid particles be calculated. Maxwel[9] derived an equation which described the thermal conductivity of a mixture of two phases of properties K_c (continuous) and K_d (discontinuous)

$$K = K_c \left[\frac{K_d + 2K_c - 2\chi_d (K_c - K_d)}{K_d + 2K_c + \chi_d (K_c - K_d)} \right] \tag{A5}$$

where χ_d is the concentration of the discontinuous material. Substituting our previous notations, $K_c = K_f$ for the fluid, $K_d = K_s$ for the solid particles and $\chi_d = 1 - \sigma$, eqn. A5 can be written:

$$K_{e,s} = K_f \left[\frac{3K_s - 2\sigma (K_s - K_f)}{3K_f + \sigma (K_s - K_f)} \right] \tag{A6}$$

Inserting this expression in eqn. A3 and replacing $(\text{Pe})_o$ and $(\text{Pe})_{\varepsilon,o}$ by their values gives the simplified equation:

$$E = \left\{ \alpha_f \left[\frac{3K_s - 2\sigma (K_s - K_f)}{3K_f + \sigma (K_s - K_f)} \right] + \sigma\alpha_f + \varepsilon \right\} \frac{1}{U_o D} \tag{A7}$$

It is noted that the particle diameter, D_p, has dropped out which is due to the fact that the dimensionless parameter S_n was neglected in eqn. A2.

For the case of water flowing at 1 ml/min into a packed column, one can evaluate E by substitution of the following thermal properties: $K_f = 1.43 \times 10^{-3}$ cal/cm · sec · °C; ϱ (density of fluid) = 1.0 g/ml; C_p (specific heat of fluid) = 1.0 cal/g · °C; $\alpha'_1 = K_f/\varrho C_p = 1.43 \times 10^{-3}$ cm²/sec: thermal conductivity of fused silica, $K_s = 3.70 \times 10^{-3}$ cal/cm · sec · °C; $\sigma = 0.53$; $U_o = Q/A = (1/60) \times 4/(0.4)^2 = 0.133$ cm/sec (Q = flow-rate; A = cross-sectional area of tube); $\varepsilon = 1.5 \times 10^{-5}$ cm²/sec. Inserting the above values in eqn. A7 yields:

$$E = (2.26 \times 10^{-3} + 7.58 \times 10^{-4} + 1.5 \times 10^{-5})/0.133 \times 0.4 \tag{A8}$$

$$= 0.0570$$

The first term in eqn. A8, which involves the equivalent thermal conductivity, is seen to be predominant. Using the above value for E the temperature profile of the fluid at the entrance of the column was calculated for r/R = 0, 0.25, 0.5 and 0.75 assuming a constant wall temperature t_w = 40°C and an inlet fluid temperature of 25°C. The resulting temperature profile is shown plotted in Fig. A1. It is seen that it takes about 1.5 cm for the fluid temperature to come to equilibrium with the wall temperature.

The data of Fig. A1 was replotted in Fig. A2 to show the radial temperature gradients at different distances χ from the entrance.

TABLE AI

THERMAL PROPERTIES OF COMMON HPLC SOLVENTS

Solvent	K_f *(cal/cm · sec · °C)*	ϱ *(g/ml)*	C_p *(cal/g · °C)*	α_f *(cm²/sec)*
Hexane	3.29×10^{-4}	0.659	0.542	9.21×10^{-4}
Methanol	4.83×10^{-4}	0.787	0.608	1.01×10^{-3}
Dichloromethane	2.91×10^{-4}	1.317	0.284	7.77×10^{-4}

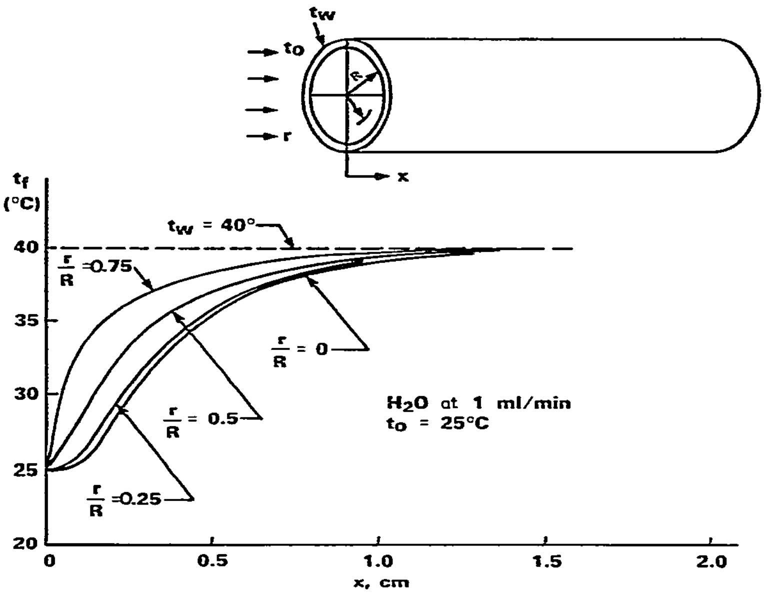

Fig. A1. Theoretically predicted radial thermal gradient in packed silica column. χ = Axial coordinate; r = radial coordinate; R = inner radius of column; t_0 = inlet fluid temperature = 25°C; t_w = wall temperature = 40°C; t_f = temperature of fluid in column at given (r, χ) coordinates. Mobile phase: water; flow-rate 1 ml/min.

It is of interest to examine the manner in which other solvents behave in comparison with water. Table AI gives the values of the properties that were used for that purpose.

The resulting values for E are given below for hexane

$$E = (2.499 \times 10^{-3} + 4.88 \times 10^{-4} + 1.5 \times 10^{-5})/0.133 \times 0.4 = 0.0564$$

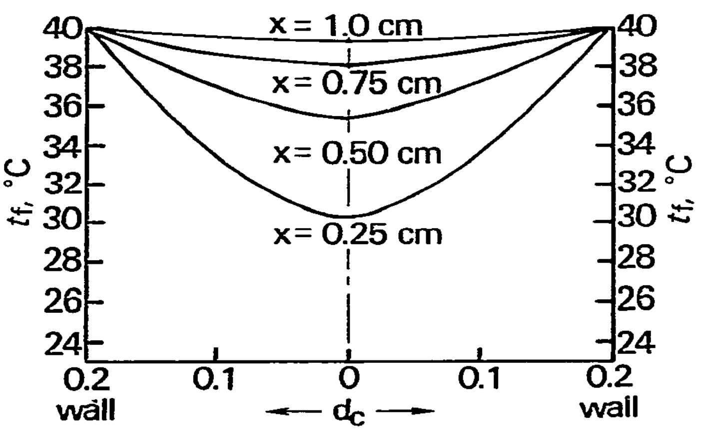

Fig. A2. Radial thermal profiles at different points along column length, χ. d_c = Column diameter; t_0 = 25°C; t_w = 40°C. Mobile phase as in Fig. A1.

for methanol

$$E = (2.463 \times 10^{-3} + 5.35 \times 10^{-4} + 1.5 \times 10^{-5})/0.133 \times 0.4 = 0.0566$$

and for dichloromethane

$$E = (2.171 \times 10^{-3} + 4.12 \times 10^{-4} + 1.5 \times 10^{-5})/0.133 \times 0.4 = 0.0488$$

It is interesting to note that even though there are significant differences between the properties of water and those of the other solvents there is but a slight difference in the resulting values of E which determines how fast the fluid will heat up. This is due to the fact that the dominant factor in E is the first term which is controlled to a large extent by the thermal conductivities of the solid silica particles.

APPENDIX II

Heating of a fluid inside a narrow bore tube with constant wall temperature

The solution of this problem is of interest for the determination of the length of tubing required to pre-heat the mobile phase to a given temperature prior to entering the column. The problem will be solved using the dimensionless approach developed by Kays and London[7] for compact heat exchangers. The assumption will be made that the tubing is in good thermal contact with a heater block and that the inner wall of the tube is thus at constant temperature. It is first necessary to determine the heat transfer coefficient across the laminar layer. An empirical correlation due to Hausen[8] is applicable to the case of laminar flow in a circular tube with constant wall temperature

$$\mathrm{Nu} = 3.65 + \frac{0.0668\,(d/l)\,\mathrm{RePr}}{1 + 0.04\,[(d/l)\,\mathrm{RePr}]^{2/3}} \tag{A9}$$

where

$\mathrm{Nu} = hd/K$ = average Nusselt number over the length l, dimensionless
h = heat transfer coefficient, $\mathrm{cal/cm^2 \cdot sec \cdot {}^\circ C}$
d = inside tube diameter, cm
K = thermal conductivity of fluid, $\mathrm{cal/cm \cdot sec \cdot {}^\circ C}$

$$\mathrm{Re} = 4Q\varrho/\pi d\eta = \text{Reynolds number} \tag{A10}$$

$$\mathrm{Pr} = \eta C_p/K = \text{Prandtl number} \tag{A11}$$

Q = flow-rate, ml/sec
ϱ = fluid density, g/ml
η = fluid dynamic viscosity, poise
C_p = fluid specific heat, $\mathrm{cal/g \cdot {}^\circ C}$

Once the heat transfer coefficient has been determined, the number of heat transfer units, Ntu, can be calculated. This is a non-dimensional expression of the "heat transfer size" of the exchanger and is given by

$$\mathrm{Ntu} = Ah/C_m \tag{A12}$$

where

A = heat transfer area, cm^2

$$C_m = Q\varrho C_p = \text{fluid capacity rate, cal/sec}\cdot{}^\circ\text{C} \tag{A13}$$

Finally, the heat transfer effectiveness, ε, is calculated from which the temperature of the fluid at any point along the tube can deduced. For a constant wall temperature the relation between Ntu and ε is

$$\varepsilon = 1 - e^{-\mathrm{Ntu}} \tag{A14}$$

and furthermore

$$\varepsilon = (t_2 - t_1)/(t_w - t_1) \tag{A15}$$

where

t_1 = entrance fluid temperature, °C
t_2 = fluid temperature at distance l from entrance, °C
t_w = wall temperature, °C

The first HPLC system to consider is that of hexane flow since hexane, having a low thermal conductivity and low thermal diffusivity, can be expected to be more slowly heated than aqueous solvents and thus constitutes a worst case example. Assume a flow-rate of 1 ml/min inside a stainless steel tube having an internal diameter of 0.23 mm. Hexane physical properties are: C_p = 0.542 cal/g·°C; ϱ = 0.659 g/ml; η = 0.00313 poise; $K = 3.29 \times 10^{-4}$ cal/cm·sec·°C; Re = 194; Pr = 5.16. Using these values the Nusselt number and heat transfer coefficient are then calculated for various lengths of tubing and the corresponding number of heat transfer units, heat transfer effectiveness and temperatures are determined. For instance at l = 5 cm: $(d/l)\cdot\mathrm{Re}\cdot\mathrm{Pr} = 4.60$; Nu = 3.65 + 3.93; h = 0.056 cal/cm^2·sec·°C; $C_m = 5.95 \times 10^{-3}$ cal/sec·°C; $A = \pi dl = 0.361$ cm^2; Ntu = 3.40; ε = 0.966.

The fluid temperature can now be calculated for any desired fluid inlet and wall temperature. Taking for example t_1 = 20°C and t_w = 70°C the fluid temperature at l = 5 cm can be calculated from eqn. A15:

$$t_2 = t_1 + \varepsilon(t_w - t_1) = 68.3^\circ\text{C}$$

Similar calculations have been carried out for different points along the tube and for wall temperatures of 30°C and 50°C. The results are shown plotted in Fig. A3A.

Another set of temperature profiles was calculated for hexane at a flow-rate of 2 ml/min and these data are shown plotted in Fig. A3B. It can be seen that in the worst case, that of hexane flow at 2 ml/min and a wall temperature of 70°C, a length of tubing of 12 cm is sufficient to raise the fluid temperature to within 1°C of the final temperature.

For comparison purposes, the heating behavior of water under the conditions

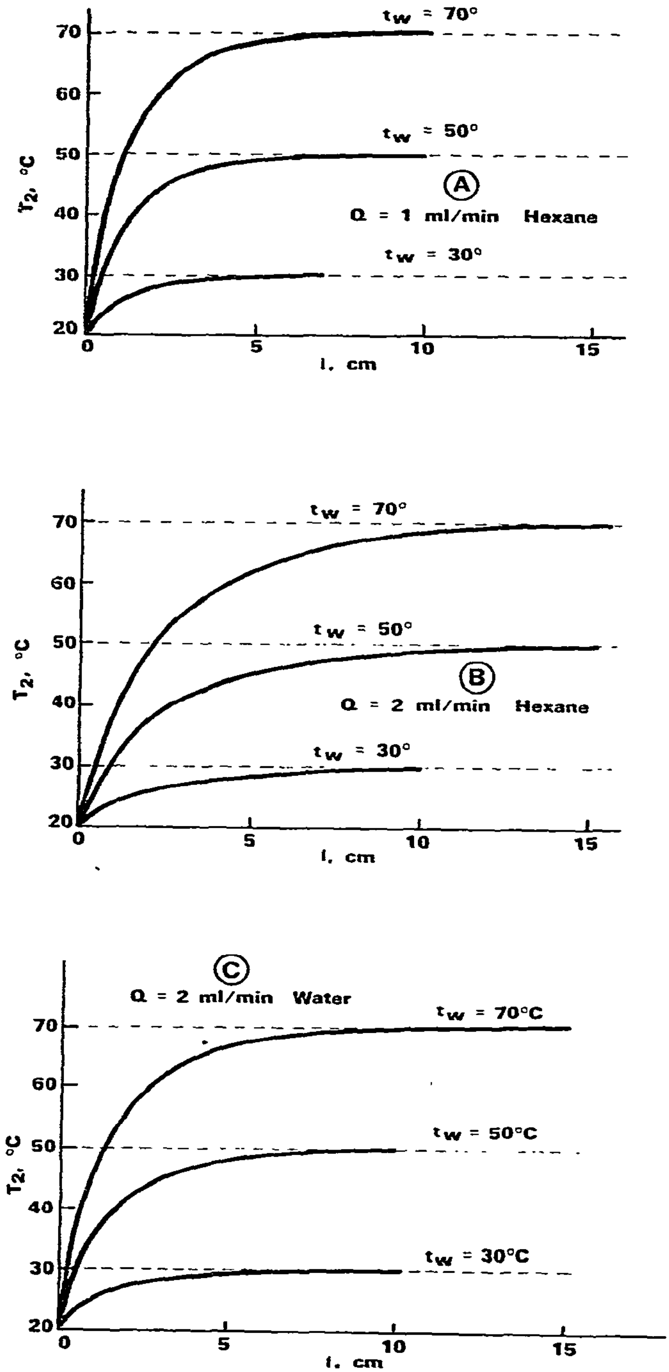

Fig. A3. Fluid temperature t_2, at a distance l from the tube inlet for a narrow bore tube, inside heater block. t_w = Wall temperature = heater block temperature. Inlet fluid t = 20°C. Mobile phases: 1 ml/min hexane (A); 2 ml/min hexane (B); 2 ml/min water (C).

previously described for hexane has been estimated using the following average properties: $C_p = 1.0$ cal/g·°C; $\varrho = 1.0$ g/ml; $\eta = 0.01$ poise; $K = 1.43 \times 10^{-3}$ cal/cm·sec·°C. The calculated profiles for water at 2 ml/min are shown plotted in Fig. A3C. It can be seen that in the worst case, that of $t_w = 70$°C, a length of only 7.5 cm of tubing is required to raise the fluid temperature to within 1°C of the final temperature.

APPENDIX III

Theoretical estimate of H(T) for RPC of anthracene

The theoretical values of Fig. A1 were obtained using the Knox equation

$$h = Av^{0.33} + (B/v) + Cv \tag{A16}$$

where

h = reduced plate height = H/D_p
v = reduced velocity = ud_p/D_m
A = eddy diffusion constant
B = longitudinal diffusion constant
C = mass transfer term constant

For example, the $h(v)$ plot of the columns studied was approximated by the Knox equation using values of 1.23, 2.8 and 0.04 for the A, B, C parameters of the 10-μm column.

The diffusion coefficient D_m was estimated by assuming $D_m \approx 1 \times 10^{-5}$ cm^2/sec for anthracene at 20°C in the mobile phase (70% acetonitrile–30% water) and the relationship:

$$D_m \propto \frac{T}{\eta} \text{ (from Wilke–Chang equation, } T \text{ in °K, } \eta \text{ in poise)}$$

The relative viscosity at each temperature was obtained from the experimental data of column pressure as f(T). Thus, one calculates $D_m(T)$ and by insertion into eqn. A16 derives H(T) for the experimental condition of $u = 0.25$ cm/sec (1 ml/min on 4 × 300 mm column).

REFERENCES

1 J. H. Knox, G. R. Laird and P. A. Raven, *J. Chromatogr.*, 122 (1976) 129.
2 I. Halász, R. Endele and J. Asshauer, *J. Chromatogr.*, 112 (1975) 37.
3 M. Martin, C. Eon and G. Guiochon, *J. Chromatogr.*, 108 (1975) 229.
4 E. Singer and R. H. Wilhelm, *Chem. Eng. Progr.*, 46 (1950) 343.
5 M. Leva, *Ind. Eng. Chem.*, 39 (1947) 857.
6 M. Leva and M. Grummer, *Ind. Eng. Chem.*, 46 (1948) 415.
7 W. Kays and A. L. London, *Compact Heat Exchangers*, McGraw-Hill, New York, 2nd ed., 1964.
8 H. Hausen, *Verfahrenstechnick, Beih. Z. Ver. deut-Ing.*, 4 (1943) 91.